Correlations between Spectroscopic, Electrochemical, and Kinetic Properties of Cyano-Bridged Binuclear Complexes. Analyses of Temperature, Pressure, and Solvent Effects

Dimitri E. Khoshtariya,*,† Hari C. Bajaj,‡ Peter A. Tregloan,§ and Rudi van Eldik*,||

Institutes of Molecular Biology & Biophysics and Inorganic Chemistry & Electrochemistry, Georgian Academy of Sciences, Gotua 14, Tbilisi 380060, Georgian Republic, Central Salt and Marine Chemicals Research Institute, Gijubhai Bedhaka Marg, Bhavnagar 364002, India, School of Chemistry, The University of Melbourne, 3052 Parkville, Australia, and Institute for Inorganic Chemistry, University of Erlangen-Nürnberg, Egerlandstrasse 1, 91058 Erlangen, Germany

Received: June 14, 1999; In Final Form: October 15, 1999

Several asymmetric cyano-bridged mixed-valence binuclear complexes were studied using electrochemical (square wave and cyclic voltammetry), spectroscopic (UV−vis−NIR absorption and ^{1}H NMR), and kinetic (stopped-flow) techniques, with special attention to the correlations between thermodynamic and optical charge-transfer characteristics determined through the variation of temperature and pressure. The CN-bridged isomers for representative EDTA-ligated complexes, viz., $[(EDTA)Ru^{III}(\mu\text{-}CN)M(CN)_x]^{5-}$ ($M = Fe^{II}$, $x = 5$; $M = Mo^{IV}$, $x = 7$), were synthesized and characterized and shown to exhibit essentially different electrothermodynamic and optical charge-transfer parameters compared to "normal" isomers. The binuclear complex-formation kinetics, spectroscopic and preliminary ^{1}H NMR data indicate that at least two EDTA ligand conformer states are formed in the course of the dimerization process studied. Using the difference DO-D stretching overtone spectroscopy of heavy water acting as solvent, it was shown that the change in hydrogen-bonding order of specifically solvating water molecules present in the first solvation shells around the redox centers may be largely responsible for the observed dramatic changes in electrothermodynamical and optical characteristics upon the variation of the nature of the ligands and their conformer (EDTA) or bridging-isomer (μ-CN) states.

1. Introduction

The increasing interest in research on cyano-bridged binuclear and polynuclear mixed-valence complexes is a result of their unique structural, redox, spectroscopic, and charge-transfer properties,[1−8] ensuring their potential application within the fields of solar energy conversion and molecular electronics.[6,9−11] The efficiency of optical or thermal intersite electron transfer in various ion−molecular aggregates, including those in the present study, is determined in particular by the redox parameters of participating electron-trapping metal centers.[3,5,7] In turn, the redox characteristics of the latter vastly depend on the nature of the first coordination sphere (the ligand composition),[7,12] and the close environment (specific interactions within the first solvation sphere) of the metal ions involved,[13,14] as well as on the macroscopic polar characteristics of the bulk solvent (resulting in continuum electrostatic solvation).[7,15] Hence, in principle, the redox and coupled optical and kinetic properties of mixed-valence clusters can be effectively tuned by selection of the appropriate ligand and/or solution composition.[7,9,12] This requires systematic studies of contributions arising from each of the above-mentioned three factors. However, discrimination between these contributions and their effect on the redox properties of metal redox centers at the quantitative level is a rather complicated task due to the overall complex character of the phenomenon.

Previous investigations have revealed that the redox properties of individual metal centers undergo significant modification as a result, in particular, of formation of binuclear or polynuclear ligand-bridged complexes due to charge delocalization effects.[7,9] The charge delocalization effect on the electrochemically determined ground-state energy, characterized by the half-wave redox potential of the *i*th species (metal center), could be presented as a sum of corrections to the corresponding ionization and solvational energy terms, respectively, summarized in eq 1:

$$\Delta E_{1/2}^{(\mathrm{deloc})} = E_{1/2}^{\mathrm{d}} - E_{1/2}^{\mathrm{l}} = -[(E_i^{\mathrm{d}} - E_i^{\mathrm{l}}) + (\Delta G_{\mathrm{s}}^{\mathrm{d}} - \Delta G_{\mathrm{s}}^{\mathrm{l}})]/F \quad (1)$$

where E_i is the ionization energy of the *i*th redox center in a vacuum, before (l) and after (d) the complexation leading to the electron delocalization, ΔG_s is the solvation free energy of the same center before (l) and after (d) the complexation, and F is the Faraday constant. Equation 1 is applicable provided that, after formation of the multicenter system, the redox centers could still be considered as redox-independent sites. The correction to the solvational energy, eq 1, in this particular case results from delocalization effects as a result of some redistribution of electron density and, consequently, a change in charge type from that of the reference state.[7]

The above-mentioned solvational effects should be distinguished from those that involve solvent molecules in the first

* To whom correspondence should be addressed.
† Georgian Academy of Sciences. E-mail: Dimitri@biophys.acnet.ge.
‡ Central Salt and Marine Research Institute.
§ University of Melbourne.
|| University of Erlangen-Nürnberg. E-mail: vaneldik@chemie.uni-erlangen.de.

10.1021/jp9919563 CCC: $19.00
Published on Web 05/12/2000

coordination sphere of metal centers. However, in certain cases, such as for aquated iron or similar metal−aqua complexes, the solvent itself forms the first coordination sphere and the separation of its contribution from that of the second sphere is even more difficult. The formal half-wave potentials of isolated (free) or binuclear and polynuclear (ligand-bridged) metal redox centers on their own are very sensitive toward the solution composition and frequently display dramatic temperature and pressure variations manifested via corresponding entropy and volume (electrostriction) effects.[15,16] Similar to the absolute values of formal redox potentials, the latter contributions can also undergo significant changes upon ligand bridging.[7,9] For isolated complex ions, attempts to rationalize these data on the basis of Born-type equations (which do not account for specific solute/solvent or solute/solute interactions)[7,15,16]

$$\Delta G_s = -(e^2Z^2N/r_{eff}D)f \qquad (2)$$

(where Z is the net charge on the redox center, r_{eff} is the effective radius, e is the electronic charge, N is the Avogadro number, D is the dielectric constant, and f is a function of the solvent independent of temperature) and

$$\Delta S_s = (e^2N/2r_{eff}DT)\,[\mathrm{d}(\ln D)/\mathrm{d}T]\,(Z_{ox}{}^2 - Z_{red}{}^2) \qquad (3)$$

$$\Delta V_s = (e^2N/2r_{eff}D)\,[\mathrm{d}(\ln D)/\mathrm{d}P]\,(Z_{ox}{}^2 - Z_{red}{}^2) \qquad (4)$$

(in which T is the absolute temperature, and P is the pressure), do not give satisfactory results without invoking the concept of specific solute/solvent interactions, manifested as a correlation with the solvent acceptor number.[13−15] It should also be mentioned here that the solvational entropy and volume contributions are only part of the overall entropy and volume changes accompanying the redox transformation of a given center. For the overall entropy and volume changes accompanying electron transfer from/to a given redox center ("half-reaction" entropy and volume, see also section 3 below) one can write[3a]

$$\Delta S_{rc}{}^o = \Delta S_{in} + \Delta S_s \qquad (5)$$

and

$$\Delta V_{rc}{}^o = \Delta V_{in} + \Delta V_s \qquad (6)$$

where ΔS_{in} and ΔV_{in} are the entropy and volume contributions connected with intrinsic changes within the redox centers (at the given state of electron delocalization), such as metal to ligand bond length, or vibrational frequency changes, etc. In the case of radial expansion/collapse of the complex redox center with pressure, for example, the change in intrinsic volume may be given by eq 7

$$\Delta V_{in} = 4/3\pi\,(r_{eff} + \Delta r)^3 - 4/3\pi r_{eff}{}^3 \qquad (7)$$

where Δr is the change in the effective radius of the redox center. A limited number of existing literature data (for binuclear compounds available on ΔS_{rc} only) indicate that the parameters ΔS_{rc} and ΔV_{rc}, determined experimentally for a given redox center, could be altered significantly when binuclear or polynuclear complexes are formed from the isolated (free) species, and that the solvational (outer-sphere) contribution should be mainly responsible for these entropy and volume effects. The metal/ligand interaction (inner-sphere) term seems to be of minor importance for the most interesting cases to be considered later.[15,16] At the same time, results of earlier studies point to the significant or even predominant role of specific solute/solvent and solute/solute interactions in the close environment (first solvation sphere) of isolated hexaammine- and hexacyanometal complex ions or their ligand-bridged derivatives, compared to the continuum-type solvation effects.[13,14] Combined formalistic approaches fail to explain, for example, that the redox entropies and volumes for structurally very similar hexaaqua- and hexaamminemetal complexes (e.g., $Ru^{II/III}$) are very different, but are rather close (in absolute values, due to the opposite charge states) for hexaqua- and hexacyanometal (ΔS_{rc}) and for hexaammine and hexacyano (ΔV_{rc}) complexes, respectively.[15,16] At the same time, ΔS_{rc} is very different for hexamine- and hexacyanometal complexes.[15] Obviously, involvement of new structural and time-resolved data on the solute/solvent interactions at the molecular level is required for the further elucidation of the role of specific hydrogen-bonding and interionic (Coulombic) interaction in the first solvational spheres of isolated and ligand-bridged metal complexes.

Contemporary charge-transfer theory establishes the linkage between the optical charge-transfer band and the redox characteristics (including the corresponding entropy and volume contributions) of electron-trapping centers involved (see the following section).[17,18] In this context, to obtain new data on temperature and pressure effects on the formal potentials of ligand-bridged redox centers seems to be of exceptional importance, since from electrochemical data the free energy gap contribution to the characteristics of the corresponding MMCT optical band could be calculated independently and compared to the results of direct spectroscopic measurements, providing new possibilities for a rigorous testing of modern theoretical models for charge transfer. Recently, new trends within the field of polynuclear ligand-bridged complex chemistry and related areas have emerged which, in combination with the above-discussed spectroscopic and electrochemical studies, can open some new prospects for a rigorous understanding of the role of fine inter- and intramolecular interactions in the course of redox processes. Several interesting examples of binuclear or polynuclear complexes were reported recently, encompassing different cyano-bridged isomers (see ref 9 for a recent review).

In addition, examination of complex ions containing chained organic ligands such as EDTA, for which different conformer states could be involved simultaneously,[19,20] can be of particular interest. One could suppose that different conformer states might differ in their ability to form hydrogen bonds with the solvating water, or other species present in the close environment, and can show up as different redox or spectroscopic characteristics. The situation here should be analogous to one with the biomacromolecules containing the metal chromophore (e.g., myoglobin or cytochrome *c*), for which the involvement of protein isomers was registered via the inhomogeneously broadened Soret bands.[21,22] The difference O−D overtone spectroscopy of heavy water was recently shown to be a useful method for study the of hydrogen bonding redistribution as a function of temperature or ion solvation.[23] However, the method is restricted to rather concentrated solutions of electrolytes to be explored (above ca. 0.3 M). Nevertheless, preliminary studies indicated that it can give valuable information about fine solute/solvent interactions in different redox states, at least for well-soluble simple (isolated) hexacyano- and hexaminemetal complexes. It seemed also likely that a combined use of bridge isomer and ligand conformer states in the context of entropy and volume effects could provide additional information about the specific solute/solvent hydrogen-bonding interactions.

In the present study, the asymmetric binuclear cyano-bridged complexes

$$[(EDTA)Ru^{III}(\mu\text{-}NC)Fe^{II}(CN)_5]^{5-} \quad (I)$$

and

$$[(NH_3)_5Ru^{III}(\mu\text{-}NC)Fe^{II}(CN)_5]^{-} \quad (II)$$

described in earlier studies[3,4] (the most fundamental features of which were reproduced also in this study, see section 3), as well as some homologous compounds and cyano-bridged isomers, were systematically investigated in more detail, including a study of temperature and pressure effects on the MMCT bands and on the formal redox potentials of the component metal centers. Difference heavy water O−D overtone spectroscopy was applied to elucidate the role of the first hydration shell water, hydrogen-bonded to the cyanoferrate and amineruthenate component ions of the cyano-bridged binuclear complexes. Some kinetic studies on the formation of the binuclear complex (I) in different water−alcohol mixtures were also performed, and the results together with optical and preliminary ^{1}H NMR data on the Ru^{III}(EDTA) moiety are discussed in the context of possible participation of different EDTA conformers in both binuclear complex formation and optical electron-transfer processes, respectively.

2. Experimental Section

Chemicals. $RuCl_3 \cdot xH_2O$, $K_4[Ru(CN)_6]\cdot 3H_2O$, and $[Ru(NH_3)_5Cl]Cl_2$ were obtained from Aldrich and used as purchased. $K_4[Fe(CN)_6]\cdot 3H_2O$ was obtained from Merck. K[Ru(H-EDTA)Cl]·$2H_2O$[3] and $K_4[Mo(CN)_8]\cdot 2H_2O$[24] were prepared according to published procedures. All other chemicals used were of AR grade. Millipore water was used throughout the experiments.

Synthesis of $K_5[(EDTA)Ru^{III}(\mu\text{-}NC)Mo^{IV}(CN)_7]\cdot 2H_2O$. $K_4[Mo(CN)_8]\cdot 2H_2O$ (0.1 g, 0.2 mM) dissolved in a minimum volume of water was added slowly to a stirred solution (10 mL) of K[Ru(EDTA)Cl]·$2H_2O$ (0.1 g, 0.2 mM) at room temperature. The color of the solution immediately changed to green. The reaction mixture was stirred for 30 min at room temperature and then concentrated in a vacuum to 2−3 mL. The desired green-colored complex was precipitated by the addition of cold acetone and filtered off. The green residue was further recrystallized twice from water−acetone mixture (3:7, v/v) and dried in a vacuum (yield 80%). CHN analysis: Found (Calc.) C, 22.07 (22.02)%; H, 2.12 (2. 03)%; N, 13.90 (14.28)%.

Synthesis of the Cyano-Bridge Isomer of (I). To 0.1 g (0.2 mM) of K[Ru(EDTA)Cl]·$2H_2O$ dissolved in 5 mL water, 0.011 g (0.225 mM) of NaCN dissolved in a minimum amount of water was added. The solution was stirred for 15 min. During this time the light brown $[Ru(EDTA)CN]^{2-}$ complex was formed. To this solution 0.07 g (0.2 mM) of $Na[Fe(CN)_5(NH_3)]\cdot 3H_2O$ was added, and the mixture was further stirred for another 30 min. Then cold acetone was added to precipitate the desired complex in which the carbon atom of the bridging cyanide is coordinated to the Ru(III) center. The green precipitate was filtered through a G-4 crucible and washed with a water−acetone mixture until it was free of Cl^-. CHN analysis: Found (Calc.) C, 23.51 (23.59); H, 1.75 (1.72); N, 13.71 (13.76), yielded results similar to those for the normal isomer.[3c]

Optical Measurements. Absorption spectra in the VIS/NIR were recorded on a Cary 5 spectrophotometer equipped with temperature controller. The high-pressure measurements were carried out using the homemade cell holder and the pillbox cell.[25] The O−D overtone spectra of heavy water in the near-IR were recorded on the Cary 5 instrument using 2 mm quartz cells (Hellma) in a single-beam mode. The difference spectra were obtained using the background subtraction and intensity normalization procedures (the latter results from temperature-induced density changes) provided in the Cary 5 software (see ref 23 for more experimental and other details).

Electrochemical Experiments. Cyclic and square-wave voltammetry was performed using a PAR 273A instrument. The three electrode nonisothermal cell configuration, consisting of a 0.5 mm platinum or gold wire working electrode, platinum wire auxiliary electrode, and a $Ag/AgNO_3$, KNO_3 reference electrode, was used throughout the temperature dependence study.[3] The high-pressure voltammetric technique was performed as described elsewhere.[16] A platinum wire (0.5 mm) working electrode was used in the high-pressure experiments. The concentration of complex ions was typically 1 mM (in the high-pressure studies 5 mM) in 0.1 M KNO_3 as supporting electrolyte. Square-wave voltammetry, which was proven earlier as a most sensitive method for the characterization of redox-active species in solution,[7,8] was also applied to test the purity of the μ-isomeric components explored in this study (see section 3).

Kinetic Measurements. These were performed on Durrum D110 or Applied Photophysics model SX.18 MV stopped-flow instruments (dead-time: ca. 5 ms). The kinetics of binuclear complex formation between $[Ru^{III}(EDTA)(H_2O)]^-$ and $[Fe^{II}(CN)_6]^{4-}$ was followed in different regions of the emerging MMCT band (see section 3 for details). Throughout all kinetic experiments a pH of 5 and ionic strength of 0.075 (when studying the solvent effects) or 0.5 M (aqueous solutions, when studying the effect of EDTA-conformer states) was maintained by using an acetic acid−acetate buffer and KCl (in the latter case), respectively. In typical experiments, pseudo-first-order conditions were selected (10-fold excess of $[Fe(CN)_6]^{4-}$), and the corresponding first-order plots were linear for at least 2−3 half-lives of the reaction. Rate constants reported are an average of at least three kinetic runs reproducible to ±4%.

3. Results and Discussion

MMCT Spectroscopy and Electrothermodynamics. The results obtained together with some earlier literature data for temperature and pressure effects on the MMCT bands for binuclear cyano-bridged complexes of present interest are collected in the Table 1. Electrochemical data for the formal redox potentials of the component redox centers in the free and binuclear configurations are also presented. Figures 1 to 3 report, for the first time, the data for the effect of pressure on the MMCT bands of cyano-bridged binuclear complexes (I) and (II), including effects on the band maximum position (Figure 2), and the absorption intensity (Figure 3), respectively. Figure 4 illustrates the effect of pressure on the half-wave potentials of the Ru and Fe redox centers, respectively, for the binuclear complex (I). For comparison, the effect of pressure on the formal potential of the free iron hexacyano complex, present in solution as an internal standard, is also presented. In contrast to the nonisothermal electrochemical cell configuration, for which the temperature effects on the half-cell potential of a reference electrode and the corresponding entropy contribution is basically excluded,[3] in the case of the high-pressure cell, the measured potential is a cell potential that includes the contribution from the effect of pressure on the reference electrode.[16] The presence of the free $[Fe^{II}(CN)_6]^{4-}$ complex as internal standard allows for a correct estimation of the formal potentials for the cyano-

TABLE 1: Comparative Table for the MMCT Band and Electrothermodynamic Parameters of Selected CN-Bridged Binuclear Mixed-Valence Complexes (see text for details)

complex/parameters	ν_{max} cm^{-1}	$\Delta\nu_{1/2}$ cm^{-1}	$d(\Delta G_{op})/dT$ $cm^{-1}\,K^{-1}$	$d(\Delta G_{op})/dP$ $cm^{-1}\,MPa^{-1}$	$E_{1/2}$, V vs NHE for Ru^{III}	$E_{1/2}$, V vs NHE for Fe/Ru/Mo	$d(\Delta G_{el})/dT$ $cm^{-1}\,K^{-1}$	$d(\Delta G_{el})/dP$ $cm^{-1}\,MPa^{1-}$	$\Delta S°_{rc}$ (Ru^{III}) e.u.	$\Delta S°_{rc}$ (M) e.u.	$\Delta V°_{rc}$ (Ru^{III}) $cm^3\,mol^{-1}$	$\Delta V°_{rc}$ (M) $cm^3\,mol^{-1}$
[(edta)Ru^{III} (μ-NC) $Fe^{II}(CN)_5]^{5-}$ [a]	10640[b]	4950[b]	−5.0[b]	0.97	0.025[b]	0.485[b]	−6.0[b]	1.74	0[b]	−17[b]	0.2	−21.7
[(edta)Ru^{III} (μ-CN) $Fe^{II}(CN)_5]^{5-}$ [a]	9600	5600	−1		0.110	0.415	0		36	−36		
[(edta)Ru^{III} (μ-NC) $Mo^{IV}(CN)_7]^{5-}$ [a]	11770	4900	−3.5		0.264	1.024						
	12000[c]	5000[c]										
[(edta)Ru^{III} (μ-CN) $Mo^{IV}(CN)_7]^{5-}$ [a]	9800[c]	4300[c]			0.152	0.840						
[(edta)Ru^{III} (μ-NC) $Ru^{II}(CN)_5]^{5-}$ [a]	14560[b]	5950[b]	−4.1[b]	1.07	−0.04[b]	0.90[b]	−3.5[b]		0[b]	−10[b]		
$[(NH_3)_5Ru^{III}$ (μ-NC) $Fe^{II}(CN)_5]^{-}$ [a]	10360[d]	4440	−13.5[d]	3.00	−0.07[d,e]	0.633[d,e]	−9.2[d]	2.72	3[d]	−23[d]	11.3	−21.8
$[(NH_3)_5Ru^{III}$ (μ-NC) $Ru^{II}(CN)_5]^{-}$ [a]	14660[f]	4630[f]	−14.7	3.15	−0.075[g]	0.902[g]						
			−13.0[d]									
$[Ru^{III}(edta)(H_2O)]^{-}$ [a]	*	*	*	*	0.02[b]	*	*	*	8	*	0.9	*
$[Ru^{III}(NH_3)_5(H_2O)]^{3+}$ [a]	*	*	*	*	0.04[d,g]	*	*	*	10[d,h]	*	29.5	*
$[Fe^{II}(CN)_6]^{4-}$ [a]	*	*	*	*	*	0.42[i]	*	*	*	−42[i]	*	−30.2[j]

[a] This work. Table footnotes *b* and *d*−*j* below indicate sources of earlier data available for the listed compounds. [b] Chatterjee, D.; Bajaj, H. C.; Das, A. *Inorg. Chem.* **1993**, *32*, 4049. Bajaj, H. C.; Das, A. *Polyhedron* **1997**, *16*, 3855. [c] Results of band deconvolution procedure for the mixed solution containing both isomers. [d] Dong, Y.; Hupp, J. T. *Inorg. Chem.* **1992**, *31*, 3322. [e] Forlano, P.; Parise, A. R.; Videla, M.; Olabe, J. A. *Inorg. Chem.* **1997**, *36*, 5642. [f] Burewick, A.; Haim, A. *Inorg. Chem.* **1988**, *27*, 1611. [g] Siddiqui, S.; Henderson W. W.; Shepherd, R. E. *Inorg. Chem.* **1987**, *26*, 3101. [h] Given for $[Ru(NH_3)_5Cl]^{2+/+}$. Hupp, J. T.; Weaver, M. J. *Inorg. Chem.* **1984**, *23*, 256. [i] Hanania, G. I.; Irvine, D. H.; Eaton, W. A.; George, P. *J. Phys. Chem.* **1967**, *71*, 2022. [j] Sachinidis, J. I.; Shalders, R. D.; Tregloan, P. A. *Inorg. Chem.* **1994**, *33*, 6180.

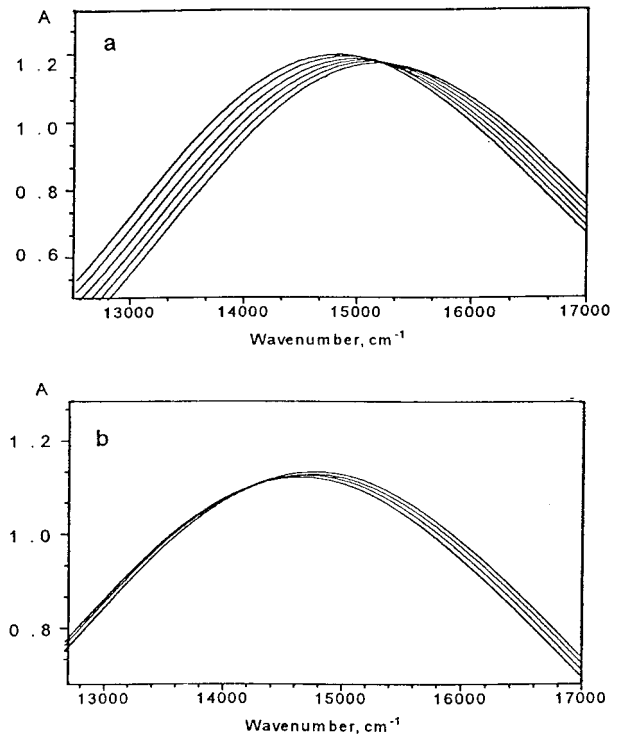

Figure 1. The effect of pressure (5−150 MPa) on the MMCT optical bands, (a) compound II, (b) compound I. Note the opposite trend in the band intensity with increasing pressure.

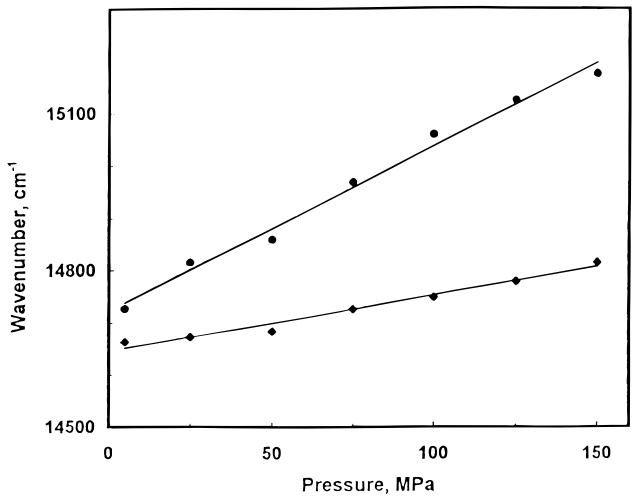

Figure 2. Change of the MMCT band maximum positions with pressure (5−150 MPa). Compound II, circles; compound I, rhombs.

bridged component metal centers by using the value of the reaction volume for the reference electrode obtained in earlier work.[16] Using the data for the temperature and pressure effects on the formal redox potentials, the composite entropy and volume parameters for the binuclear complexes were estimated with the aid of the following expressions:[3]

$$d(\Delta G_{el})/dT = -nF\, d(\Delta E_{1/2})/dT = \Delta S_{rc}^{o}(M) - \Delta S_{rc}^{o}(Ru^{III/II}) \quad (8)$$

$$d(\Delta G_{el})/dP = -nF\, d(\Delta E_{1/2})/dP = \Delta V_{rc}^{o}(M) - \Delta V_{rc}^{o}(Ru^{III/II}) \quad (9)$$

where ΔG_{el} is the free energy gap between the redox states of the metal centers forming the cyano-bridged binuclear complex,

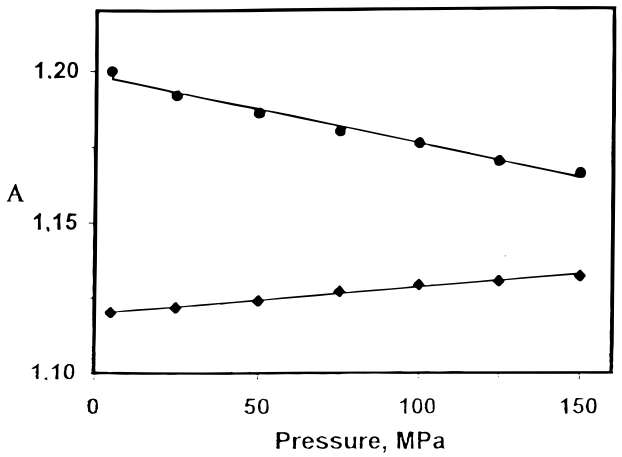

Figure 3. Change of the MMCT band intensities with pressure (5−150 MPa). Symbols are the same as in the Figure 2.

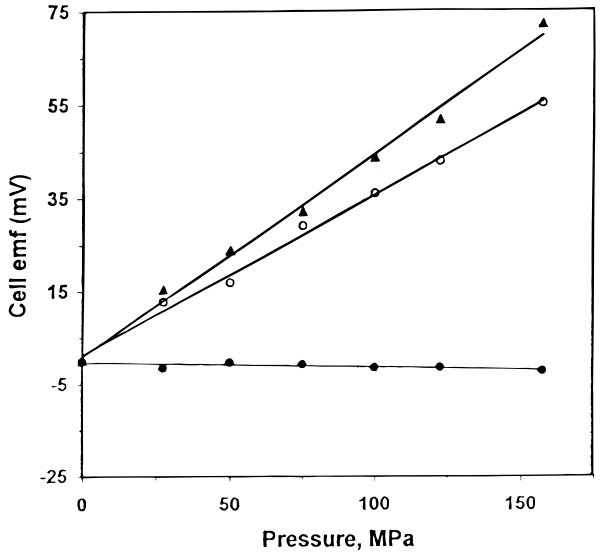

Figure 4. Effect of pressure on the half-wave potentials of Ru (closed circles) and Fe (open circles) redox centers of compound I. The effect of pressure on the formal potential of free hexacyanoferrate complex (triangles) is also presented for comparison (serving as an internal standard, see text).

$E_{1/2}$ represents the half-wave potential of the individual cyano-bridged center, and ΔS_{rc}^{o} and ΔV_{rc}^{o} are the half-reaction entropies and volumes contributed by each redox center, respectively[3,16]

$$\Delta S_{rc}^{o} = S_{red}^{o} - S_{ox}^{o} \quad (10)$$

$$\Delta V_{rc}^{o} = V_{red}^{o} - V_{ox}^{o} \quad (11)$$

According to the extended version of the Hush theory, the MMCT band maximum (free) energy, ΔG_{op}, is given by the following expression:[18]

$$\Delta G_{op} = \Delta G_{o} + \Delta G_{in} + \Delta G_{out} + \lambda_{so} \quad (12)$$

where ΔG_o is the free energy gap between the initial and final states of electron transfer, ΔG_{in} and ΔG_{out} are the inner- and outer-sphere (reactant and solvent) free energies of reorganization, respectively, and λ_{so} represents the spin−orbit coupling effects for the product state of the optical electron transfer.[18,26] From eq 5 it follows that the temperature (resulting in entropy) or pressure (resulting in volume) contributions to any factor on the right-hand side of the equation should lead to an observable temperature or pressure dependence of the MMCT band maximum energy. It was argued in earlier papers that the only parameter which can undergo significant changes with temperature (and consequently with pressure) would be ΔG_o, which could be identified with ΔG_{el} from eqs 1 and 2.[3,27] Thus, the values of $d(\Delta G_{op})/dT$ and $d(\Delta G_{el})/dT$ obtained from the independent optical and electrochemical experiments, respectively, could be directly compared with each other. From Table 1, summarizing also the earlier data on this topic, it follows that the agreement is in most cases satisfactory within the limits of the experimental errors, demonstrating the sound basis for the assumptions made above.

From recent studies by Olabe and co-workers[6] it becomes obvious that the complexes of type (I) (including Ru and Os homologues) in solution are in equilibrium with parent mononuclear complex ions. The rate constants of formation and decomposition of these complexes and corresponding equilibrium constants were calculated under ambient conditions (room temperature and atmospheric pressure).[6] Previous[3,16] and present (Figures 1 and 3) results for the temperature and pressure effects, respectively, on the MMCT band intensities indicate that the observed small but rather pronounced intensity changes should be related to corresponding changes in the concentration of absorbing binuclear complexes due to temperature- or pressure-induced shifts in the corresponding equilibria. Recently, we have recommended an approach for the estimation of equilibrium constants under different temperature and pressure conditions, and the corresponding thermodynamic contributions, on the basis of temperature and pressure studies of relevant MMCT or other intersite CT bands.[28] Experimentally determined absorption at the CT band maximum, A_m, and the equilibrium constant for the formation of a two-site associate (e.g., binuclear complex), K_A, are related via the following expression:

$$A_m = [X]\epsilon_m l = K_A([C_1] - [X])([C_2] - [X])\epsilon_m l \quad (13)$$

where $[X]$ is the actual concentration of absorbing species, $[C_1]$ and $[C_2]$ are the concentrations of reactant (parent) species, ϵ_m is the molar extinction at the band maximum, and l is the optical path length. The parameter ϵ_m is essentially independent of pressure (provided the structure of the binuclear complex is not altered) and is dependent on the temperature via the following fundamental equation[28] (in the high-temperature limit applicable here, for the original work, see ref 17, e.g.):

$$\epsilon_m = \text{const } T^{1/2} \quad (14)$$

It follows that if the values of ϵ_m and K_A are determined under the defined experimental conditions (at room temperature and atmospheric pressure, e.g.), then the equilibrium constant can easily be estimated under different temperature or pressure conditions via the determination of only A_m.[28] We have used the spectroscopic data for the temperature and pressure effects on the MMCT band (viz., on the parameter A_m) of compound (I) obtained in the previous[3] and present work (Figures 1 and 3) together with the value of $K_A = 1.4 \times 10^4$ M^{-1} ($\Delta G_A = -24$ kJ mol^{-1}), determined earlier at ambient conditions,[3] to calculate the values of ΔG_A at different temperature and pressure conditions. This then provides values for the thermodynamic parameters ΔH_A, ΔS_A, and ΔV_A, respectively (these thermodynamic parameters should not be confused with those considered in eqs 5−12). The obtained values are −4.3 kJ mol^{-1}, −65.3 J K^{-1} mol^{-1}, and +2.4 cm^3 mol^{-1}, respectively. For compound (II), the equilibrium constant of formation is not

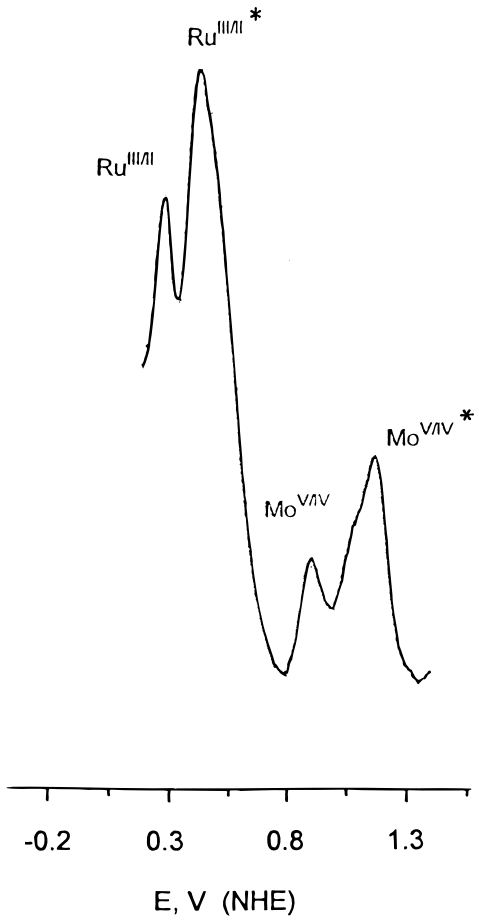

Figure 5. Square-wave voltammogram of the solution containing two μ-isomers of the cyano-bridged $Ru^{III}-Mo^{IV}$ complex. The peaks due to formal potentials of the "normal" isomer are indicated by asterisks.

available, due to the stable precursor ion-pair formation. However, variation of its value within a realistic range around $K_A = 10^5$ M^{-1} yielded reasonable thermodynamic parameters $\Delta H_A = -11.7$ kJ mol^{-1}, $\Delta S_A = -57.3$ J K^{-1} mol^{-1}, and $\Delta V_A = -2.5$ cm^3 mol^{-1}. We note opposite trends in A_m (Figures 1 and 3) with increasing pressure and opposite signs of the reaction volumes for the formation of compounds (I) and (II), respectively, while the temperature effects (and thus the enthalpy and entropy contributions) are similar. These effects are probably related to changes in hydrogen-bonding networks during the course of formation of the two different cyano-bridged complexes (see further discussion).

Cyano-bridged isomers of complex (I) and its Mo^{IV} analogue are reported for the first time. The former isomeric complex was isolated in the solid state and completely characterized in solution both spectroscopically and electrochemically (Table 1). The μ-isomer of the Ru^{III}-Mo^{IV} cyano-bridged complex was obtained in a racemic solution only, mixed with a "normal" isomer. Figure 5 illustrates electrochemical detection of both isomers in the solution. Deconvolution of the corresponding MMCT band revealed that the observed band can be viewed as consisting of two main components, satisfactorily resembling the electrochemical data (Table 1). It is worth mentioning the essentially different temperature effects on the electrothermodynamic and MMCT optical band characteristics for the two CN-bridged isomers of complex (I) (see also further discussion). The overall agreement between the two sets of results, presented in the Table 1 as ΔG_{op} (calculated directly from the spectroscopic data) and ΔG_{el} (calculated from the electrochemical data

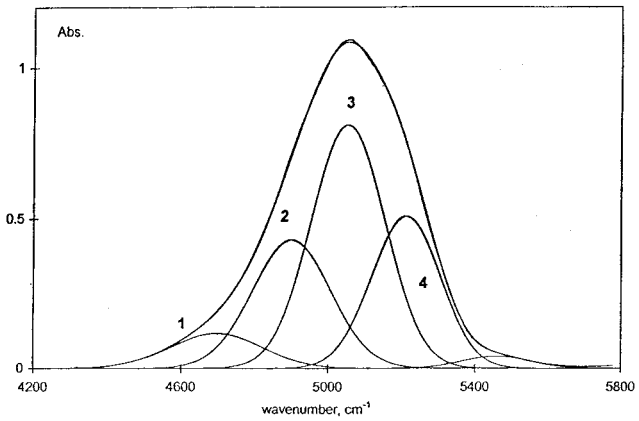

Figure 6. DO−D stretching overtone band of pure heavy water at 25 °C. Numbers indicate the deconvoluted major subbands corresponding to "ice-like" (1), "normal" (2), "bifurcated" (3), and "almost broken" (4) hydrogen-bonded states of O−D oscillators, respectively (see text for details).

and transformed into the "optical" units for comparison reasons), is satisfactory except for the case of a pressure effect for compound (I), which probably requires further refinement.

Difference O−D Overtone Spectroscopy Studies. Comparative analysis of data presented in Table 1 for temperature and pressure effects on the redox potentials of metal complex redox centers under different conditions (separated vs ion-bridged, with different ligand composition at the Ru center, and for different isomer states of the bridged cyanide) also reveal dramatic changes in both the resulting entropy and volume parameters and the corresponding individual (half-reaction) contributions, see Table 1. The large entropy and volume effects observed for the cyanometalate component while going from the free to the binuclear states are especially notable. For the Ru component, the entropy effects are relatively modest with an exception in the case of the cyano-bridged isomer, for which the half-reaction entropies of both components are changed, surprisingly, by a significant but similar extent yielding an almost zero change in the overall free energy (the result was also confirmed by the corresponding independent optical experiment, see Table 1). The analysis of previous results[23] led to the supposition that specific solute/solvent interactions, in particular modification of hydrogen-bonding networks involving the hydrogen-bond acceptor/donor ligands and solvent water, under the influence of cyano-bridged partner complex ions, could be of major importance for such effects. Hereby, we consider for the first time the hydrogen-bonding effects of hexacyano and hexa(penta) ammine metal complexes with water, for which the pressure (volume) effects are comparable but the temperature (entropy) effects are obviously different (see Table 1).

Recently, a method of difference O−D overtone spectroscopy was developed that allows the quantitative estimation of fractions of heavy water oscillators, O−D, involved in different kinds of hydrogen-bonding in the liquid phase (see below).[23,29] The method is based on the fact that the integrated intensity of the O−D oscillator absorption in the overtone (near-IR) region does not depend on the strength of a hydrogen bond in which the oscillator is involved.[23] The method was tested for the oscillator distribution in pure heavy water and was proven as a powerful quantitative approach for the determination of various water states in different systems within the detectable signal-to-noise ratio.[23] Figure 6 illustrates the O−D oscillator distribution in pure D_2O at 25 °C. According to literature,[29,30] the resulting inhomogeneously broadened vibrational bands (IR or Raman)

representing the water molecule assemblies could be presented as convolution integrals of several homogeneously broadened component bands

$$\epsilon_o(\nu) = \int_0^\infty \int_0^i N(\nu_i)\sigma(\nu_i)F(\nu_i)\, d\nu \qquad (15)$$

where $\epsilon_o(\nu)$ is the molar extinction coefficient at the wavenumber ν, $N(\nu_i)$ describes the spectral distribution function for the number density of OH (OD) subgroups with frequency ν_i, $\sigma(\nu_i)$ is a peak absorption cross section, and $F(\nu_i)$ is the homogeneous line shape function, usually assumed to be Gaussian or Lorentzian. $N(\nu_i)$ obeys the normalization condition

$$\int_0^\infty \int_0^i N(\nu_i)\, d\nu = N_o \qquad (16)$$

with a total number density N_o of OH (OD) oscillators. For pure D_2O, five component bands, tentatively attributed to the oscillators involved in "ice-like" (strong), "normal", "bifurcated" (weakened), and "almost broken" (very weak) hydrogen bonds, were deduced from previous Raman[29] and IR overtone[23] experiments (see Figure 6).

In the present study, the hexacyanoferrate(II) and -(III) species, of which concentrated solutions are sufficiently stable in both oxidation states, were selected as appropriate complex ions to study the role of solute/solvent hydrogen bonding interactions within the context of temperature and pressure effects (manifested as large reaction entropy and reaction volume contributions). Figure 7 represents (a) the difference O−D overtone spectrum of pure heavy water for two different temperatures, (b) the similar difference spectrum for pure heavy water and the 2 M KCl solution (in D_2O), and (c) the difference spectrum for two solutions containing 0.6 M $K_4[Fe^{II}(CN)_6]$ and $K_3[Fe^{III}(CN)_6]$ (in D_2O), respectively. From a comparison of Figures 6 and 7a, it can be concluded that the increase in temperature within definite intervals leads to substantial weakening ("breakage") of the corresponding amount of "normal" (but not very strong "ice-like") hydrogen bonds. In Figure 6 these fractions are indicated by numbers 2 and 4, respectively. Figure 7b reveals that dissolving 2 M KCl results in an effect very similar to a temperature rise of ca. 10 K, namely, that ca. 10% of all O−D oscillators, which could be attributed to 10% of the total (reduced) number of water molecules (see ref 23 for details), change their hydrogen-bonded state from "normal" to "almost broken". This effect is mostly due to the solvation of chloride ions, via formation of very weak hydrogen bonds with water (or heavy water), known in the literature as "structure-breaking" anions.[31] It was shown that potassium ions do not appreciably change the hydrogen-bond strength distribution of water.[23] Turning now to Figure 7c, it is seen that the difference O−D overtone spectrum, reflecting changes in the solvation sphere of hexacyanoferrate complex ions (present in 0.6 M concentration) upon a change of charge state (accompanying the redox transformation), points to the transformation of 10% of all (heavy) water molecules (corresponding to ca. six water molecules per one dissolved hexacyanoferrate ion) from very strong ("ice-like") hydrogen-bonded state, denoted in Figure 6 by number 1, to the "almost broken" condition (number 4 in Figure 6). The detailed analysis of all the difference O−D overtone spectra obtained, including the difference spectra between the pure heavy water and hexacyanoferrate(II) and hexacyanoferrate(III) solutions, respectively (to be published elsewhere[23]) allows us to conclude that six water molecules among 12 others, strongly hydrogen-bonded to

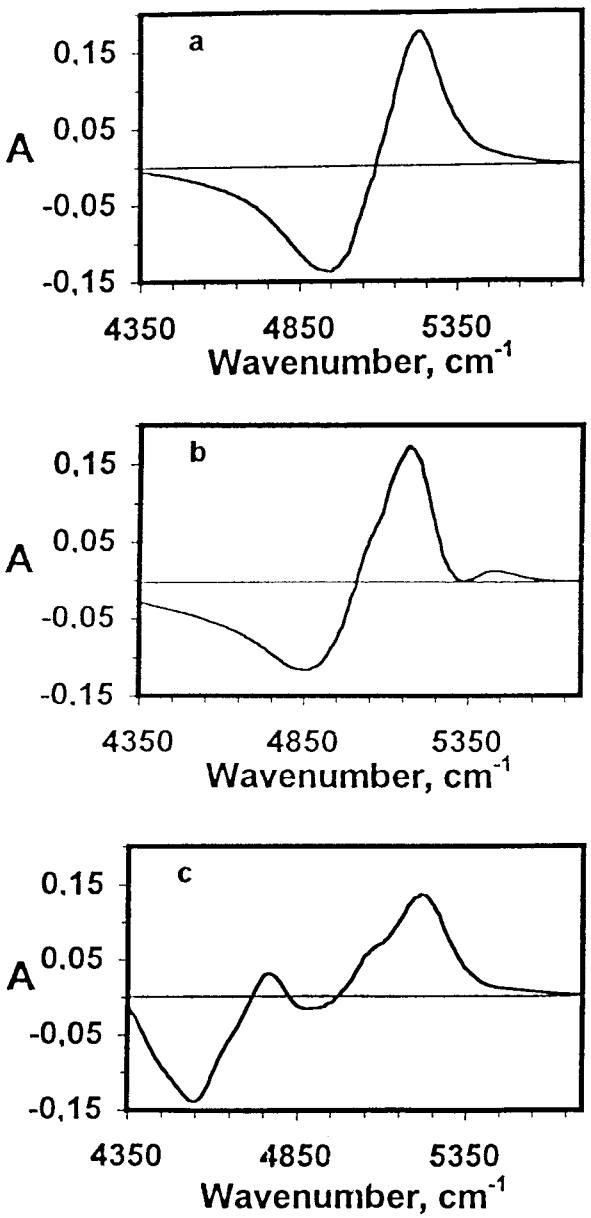

Figure 7. Difference DO−D stretching overtone spectra: (a) pure D_2O at 35° minus at 25 °C; (b) D_2O solution in 2 M KCl minus pure D_2O; (c) D_2O solutions in 0.6 M each, $K_3[Fe^{III}(CN)_6]$ minus $K_4[Fe^{II}(CN)_6]$ (see text for details).

terminal nitrogen atoms in the reduced state of the complex (forming probably linear hydrogen bonds involving the nitrogen lone-pair electrons), dramatically change their hydrogen-bonded status upon oxidation, going to the configuration of almost free rotation (dangling), keeping only very weak hydrogen-bonding interaction with hydrogen-acceptor nitrogen atoms. The entropic "costs" for the release of one water molecule through such a transformation amounts to ca. 7 e.u.[32] Hence, we conclude that the literature value of $\Delta S_{rc}^o(Fe^{III/II}) = -42$ e.u. reported for the oxidation process of free hexacyanoferrate ions dissolved in water[15] is a reflection of the arrangement (significant strengthening) of six hydrogen bonds around the complex upon its reduction.

In contrast to the hexacyanoferrate component, much smaller entropy changes are envisaged for the pentamine ruthenium component in the free or ligand-bridged states (Table 1). We have also performed difference O−D overtone spectroscopic studies of concentrated solutions containing $[Co^{III}(ND_3)_6]^{3+}$ and

$[Ni^{II}(ND_3)_6]^{2+}$ complex ions (present as 0.3 M chloride salts dissolved in D_2O), explored as model compounds imitating different redox states of the less stable $[Ru(ND_3)_5]^{3+/2+}$ component of the binuclear species of present interest. The results revealed almost no detectable difference in the O−D overtone spectra for these two solutions, which is compatible with the hydrogen-bond formation/breaking effect involving a maximum of one water molecule and the published value of $\Delta S_{rc}^{o}(Ru^{III/II}) = +10$ e.u. for $[Ru(NH_3)_5Cl]^{2+/+}$.[15] Hence, we conclude that no significant hydrogen-bond formation/breaking effects take place upon oxidation/reduction of the isolated hexa(penta)amine ruthenium component redox center. The reorganization effect of water molecules hydrogen-bonded in the first solvation sphere of free ammine metal complexes, showing up as significant reaction volume contributions (Table 1), should be connected with the linear (small on average) elongation/shortening of radially distributed hydrogen bonds without alteration in their type and geometry, as it was already discussed earlier by Lay.[13a]

On accepting now the hydrogen-bonded network effects (in particular, the hydrogen-bond formation/breakage transformations) as a major source for the appearance of entropy terms, revealed by the temperature dependence studies, it can be concluded that the observed changes in entropy contributions upon ligand-bridging with different types of counter Ru complexes (ligated by EDTA or $(NH_3)_5$) could be connected with the different character of hydrogen-bonding within the networks formed in the presence of different hydrogen-bond donor/acceptor environments. In particular, in the case of ligand-bridged complexes, cyano and amine ligands can form direct or water-implicated hydrogen-bonding networks.[33] The environmental properties of the latter can differ significantly from those of nonbridged complexes. For example, if almost half of the cyano-ligands of the binuclear complex are occupied by strong and direct hydrogen-bonding with the neighboring amine ligands, a corresponding half-contribution of the entropy will be eliminated from the value detected for a free $Fe(CN)_6$ component ion.

In the case where L = EDTA, the situation seems to be much more complicated. There are numerous indications in the literature on the ability of this ligand to attain multiple conformational substates,[19,20] as well as to form extensive hydrogen-bonded networks.[34] It is impossible to elucidate these aspects by applying the method of difference O−D overtone spectroscopy directly to the D_2O solutions containing $[Ru^{III}(edta)(H_2O)]^-$ ions, due to insufficient solubility of this compound. However, one can visualize the other manifestations of the above-discussed intrinsic features through the application of other relevant experimental techniques and via the subsequent comparative analysis of experimental data. For instance, the 10-fold difference in the binuclear complex formation rate constants between the $[Ru^{III}(EDTA)(H_2O)]^-$ species and the hexacyanoferrate complex acting in different oxidation states[3c,6d] can be ascribed to the different ability of the latter complex to form strong hydrogen bonds in these two states as discussed in this subsection (the formal charge-state of the entering ligand seems to be of minor importance for the water replacement ability at the Ru center[3,6]). Below we will discuss some other manifestations of this kind based on kinetic and NMR data.

Kinetics of Complex Formation (I): Evidence for the Involvement of Different EDTA Conformers. The kinetics of the formation of complex (I) was studied recently by several groups.[3,6] It was found that the process takes place via substitution of the aqua ligand in the $[Ru^{III}(edta)(H_2O)]^-$ complex, analogously to similar substitution reactions involving small entering ligands.[35] However, the effect of solvent composition has not yet been explored.

TABLE 2: Observed (pseudo-first-order) Rate Constants and Activation Parameters for a Slow Component of the Substitution Reaction of $[Ru(edta)(H_2O)]^-$ with $[Fe(CN)_6]^{4-}$ (formation of compound I) in Different Solvents[a]

solvent	% solvent	k_{obs}, s^{-1}	$\Delta H^{\neq}$, kJ mol^{-1}	$\Delta S^{\neq}$, J K^{-1} mol^{-1}
H_2O	100	0.066	32.5 ± 2	−156 ± 6
MeOH	10	0.126		
	25	0.176		
	35	0.45		
	50	0.73		
	60	0.88	31.8 ± 3	−140 ± 9
EtOH	42.5	1.12		
t-BuOH	1.25	0.063		
	5	0.067		
	25	0.26		
	50	1.29	37.9 ± 1.3	−115 ± 4
i-PrOH	50	1.54		
glycerol	50	0.05		

[a] Standard conditions: 25 °C, $\mu = 0.075$ M (acetate−acetic acid buffer), pH 5.0, $[Ru^{III}(edta)(H_2O)]^- = 5 \times 10^{-4}$ M, $[Fe^{II}(CN)_6]^{4-} = 5 \times 10^{-3}$ M.

To gain further information on the nature of the rate-determining step, we investigated the dependence of the rate constant of this substitution process on the solution composition under pseudo-first-order conditions in mixtures of water and methanol, ethanol, *tert*-butyl alcohol, 2-propanol and glycerol, as summarized in Table 2. The ionic strength of the solutions was adjusted to 0.075 M in order to increase the reactant solubility in water−alcohol mixtures (the quoted values are observed pseudo-first-order rate constants). We found that at higher concentrations of some alcohols (viz. *tert*-butyl alcohol, 2-propanol) under standard experimental conditions (wavelength: 870−900 nm, time-scale: 0.01−5 s) the kinetics followed an essentially two-exponential behavior, yielding rate constants that differ by a factor of 3 or more (see further discussion). The resolution of a fast component occurring mostly within the time scale of less than 5 milliseconds (i.e., dead-time of the instrument) was unsatisfactory (small amplitudes), leading to poor reproducibility of the corresponding rate constant. The rate constants representing the slower (well-resolved) kinetic component were reproducible and exhibited a gradual increase on going to the higher alcohols and to higher alcohol concentrations (Table 2). In a 50% (v/v) water−glycerol mixture, the rate constant was slightly lower compared to 100% H_2O. We reinvestigated the kinetics of the formation of complex (I) under the standard conditions and found essentially a similar situation: the "established" bimolecular rate constant of ca. 100 M^{-1} s^{-1} (25 °C) can be obtained through the one-exponential kinetics with a small amplitude (at the CT band maximum!) observable in the spectral region around 900 nm within the time-scale of 0.1−5 s. On going to shorter wavelengths (higher wavenumbers), the kinetics become essentially two-exponential and the overall amplitude increases due to the increasing contribution of the slower component exhibiting an amplitude maximum at ca. 715 nm (14000 cm^{-1}). Measurements on shorter time scales (10−100 ms) revealed that in the CT band maximum (around 900 nm) 90% of the absorbance change takes place within the first 10 ms (poorly resolved component only displayed as "tail") with a rate constant (roughly estimated) at least 3 times exceeding that reported in the literature[3,6] (determined from the slower component of the kinetic trace).

In other words, we have disclosed that two definite parts of the optical band, corresponding to the metal−metal CT transition

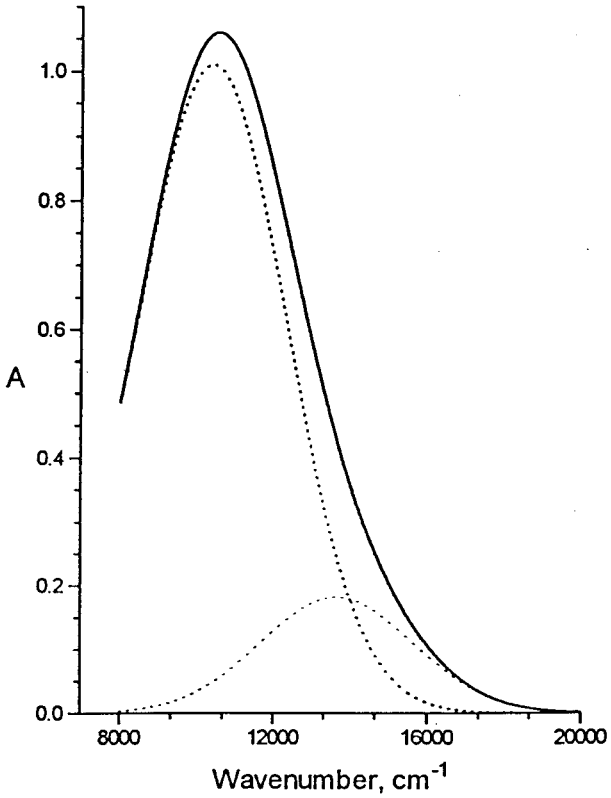

Figure 8. The MMCT band of compound I deconvoluted in two Gaussian subbands presumably representing two different major conformer states of the EDTA ligand (see text for discussion).

within the complex (I), are formed on two rather different time scales. Analyzing the signal amplitudes of the kinetic curves, we found that the slower pathway gives rise to only ca. 20% of the total final integral absorbance (i.e., only to 20% of the total amount of binuclear complexes, provided the extinction coefficients of these two fractions are similar), and that the location of larger amplitudes differs notably from that of a global maximum of the resulting MMCT band. We have performed a computer deconvolution of the resulting MMCT band of compound (I) into two Gaussian bands (see Figure 8), and the result obtained was similar to that from the analysis of the stopped-flow signal amplitudes indicating the participation of two conformer species in solution. The rate constants for the formation of compound (I) reported in earlier papers,[3,6] and obtained in the present study (presented in the Table 2) obviously correspond to that fraction of the complex with a MMCT band maximum at 14000 cm^{-1} (the slower component). One may argue that this subband corresponds to a fraction of the trinuclear complex, viz.,

$$[(EDTA)Ru^{III}(\mu\text{-}NC)Fe^{II}(CN)_4(\mu\text{-}CN)Ru^{III}(EDTA)]^{6-} \quad (III)$$

shown recently to give rise the MMCT bands at some 1500 cm^{-1} higher energy compared to the related binuclear compound (I). However, trinuclear compounds of the type (III), as reported in earlier papers,[6] can only be formed in an excess of $Ru(EDTA)(H_2O)^-$ as starting material, whereas in our optical experiments solutions were used that were prepared from the solid compound (I) (checked by elemental analysis and square-wave voltammetry, see section 2), or formed as a result of mixing in the stopped-flow instrument (under a 10-fold excess of the cyanoferrate component). Furthermore, the MMCT band maximum separation for two possible EDTA conformer-states, detected in the present study, amounts to ca. 4000 cm^{-1} (Figure 8). This value is much larger than the band maximum separation between binuclear and trinuclear species mentioned above, thus indicating that the formation of trinuclear or other higher complexes cannot be responsible for the observed effects. Moreover, extension of the time scale of the stopped-flow measurements up to 20−30 s revealed once more the slowest component for the complex-formation (I) kinetics, with a characteristic rate constant of ca. 10 M^{-1} s^{-1} (with a small amplitude throughout the whole CT band). However, the overall situation here is different from the case of the $[Fe^{II}(CN)_6]^{4-}/MV^{2+}$ ion pair formation kinetics exhibiting essentially a multiexponential pattern.[28b] The rate-determining step in that case is the outer-sphere diffusion leading to the essentially viscosity-dependent rate constant. In the present case, the rate constant is sensitive to the hydrogen-bonding ability of the cosolvent, rather than the solution viscosity (Table 2). Consequently, the rate-determining step is probably associated with a rearrangement of the hydrogen-bonded network, starting from some metastable precursor state. Formation of the precursor state is well documented for compound (II) in which case it is long-lived and easily detectable.[1,4] It seems that the high conformational lability of the EDTA ligand leads not only to the splitting of the MMCT band and the corresponding kinetic traces into two major components but also to smoother inhomogeneous dispersion of these characteristics. This can also be visualized by a comparison of the MMCT band half-widths for the complexes of type (I) and (II). From Table 1 it is seen that the EDTA-containing binuclear complexes display much broader MMCT bands compared to their pentammine analogues, indicative of broad distribution of numerous contributing subconformational states.

We have also performed a limited number of ^1H NMR measurements in order to identify the possible EDTA conformer states involved in the binuclear complexes of type (I). Unfortunately, the solubility of this binuclear compound is too low to enable direct NMR measurements. Instead, the $Ru^{III}(edta)(CN)^{2-}$ mixed-ligand complex was explored as an analogue for the cyano-bridged binuclear species. Results of tentative analysis of the ^1H NMR spectrum of this complex (recorded at pH 5, see Figure 9) are consistent with the suggestion of the involvement of different EDTA conformer states. The signal consists of a broad singlet with a maximum at 3.22 ppm, representative of four ethylene protons, and several resonances within the range of 3−4.5 ppm, representative of carboxylate protons, in general agreement with the spectra of related EDTA complexes.[20] Although the spectrum is complicated by the overlay with minor contributions of 3/2 and 5/2 spin isotopic components of the Ru moiety, three major groups of resonances due to the EDTA carboxylate groups could be determined, viz., one multiplet (which could be the overlay of two [AB] patterns) around 4.05 ppm, another multiplet around 3.7 ppm, and two singlets, located at 4.36 and 4.41 ppm, respectively. The latter, on the basis of their relative area of ca. 1:6, could be attributed to the carboxylate protons of the "free" carboxylate arm of the EDTA ligand. Two other minor singlets, which could be easily distinguished from weaker spin multiplets, are situated at 4.21 and 4.26 ppm, respectively. These could be attributed to the minor conformer state of the "free" carboxylate arm. Thus, two major conformer states of pentadentate EDTA/metal complex could be distinguished on the basis of stereochemical considerations, with equatorial and polar (axial) X-ligand (aqua, or CN^-) substituted configurations, in general accordance with the MMCT spectral and kinetic data.

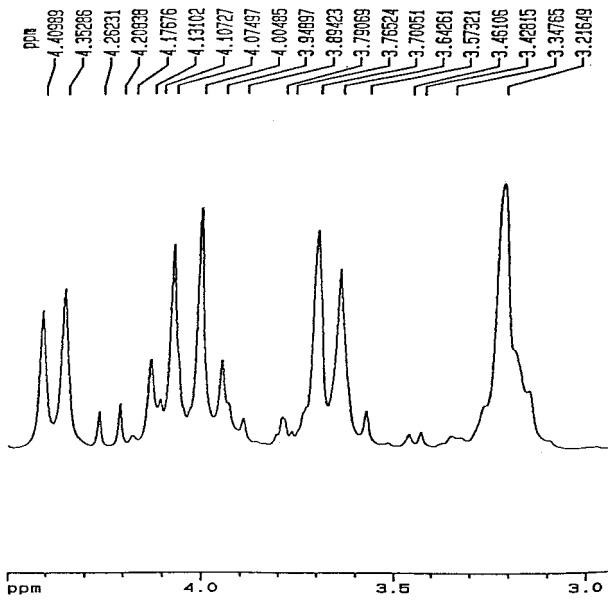

Figure 9. ^{1}H NMR spectrum (displayed over 3−4.5 ppm) of the solution containing $Ru^{III}(EDTA)(CN)^{2-}$ (with excess CN^-, pH 5, no buffer added).

In summary, we note that the large variety of results obtained in the present study strongly points to the exceptional role of the structure and reorganizational dynamics of the specifically solvating first hydration shells in redox processes with the participation of both intact ("free") complex ions and their binuclear or polynuclear derivatives. Accordingly, the formation of polynuclear aggregates involves essential rearrangement of hydrogen-bonded networks in the environment of parent ions, along with the covalent and Coulombic changes. The structure of these networks obviously is very sensitive to even the minor structural modifications of binuclear species as in the case of involvement of the CN-bridge isomers or the EDTA-ligand conformers.

Acknowledgment. D.E.Kh. is grateful to the Alexander von Humboldt Foundation for the resumption of his fellowship. DAAD fellowships for H.C.B and P.A.T. are also kindly acknowledged. The authors are indebted to Dr. A. Zahl for the performance of ^{1}H-NMR experiments and to Dr. I. Tóth for discussions concerning the NMR data. We thank Dr. A. Neubrand and Mr. P. Lindquist-Reis for the assistance in recording and processing the O−D overtone spectra.

References and Notes

(1) (a) Ludi, A. *Chimia* **1972**, *26*, 647. (b) Burewick, A.; Haim, A. *Inorg. Chem.* **1988**, *27*, 1611.

(2) (a) Vogler, A.; Osman, A. H.; Kunkely, H. C. *Coord. Chem. Rev.* **1985**, *64*, 159. (b) Scandola, F.; Argazzi, R.; Bignozzi, C. A.; Chiorbolli, C.; Indelli, M.; Rampi, M. A. *Coord. Chem. Rev.* **1993**, *125*, 283.

(3) (a) Dong, Y.; Hupp, J. T. *Inorg. Chem.* **1992**, *31*, 3322. (b) Hupp, J. T.; Dong, Y. *J. Am. Chem. Soc.* **1993**, *115*, 6428. (c) Chatterjee, D.; Bajaj, H. C.; Das, A. *Inorg. Chem.* **1993**, *32*, 4049. (d) Chatterjee, D.; Bajaj H. C.; Das, A. *Inorg. Chim. Acta* **1994**, *224*, 189.

(4) (a) Poulopoulou, V. G.; Li, Z.-W.; Taube, H. *Inorg. Chim. Acta* **1994**, *225*, 173. (b) Poulopoulou, V. G.; Taube, H. *Inorg. Chem.* **1997**, *36*, 4782.

(5) (a) Tominaga, K.; Kliner, D. A. V.; Johnson, A. E.; Levinger, N. E.; Barbara, P. F. *J. Chem. Phys.* **1993**, *98*, 1228. (b) Doorn, S. K.; Dyer, R. B.; Stoutland, P. O.; Woodruff, W. H. *J. Am. Chem. Soc.* **1993**, *115*, 6398. (c) Reid, P. J.; Silva, C.; Barbara, P. F.; Karki, L.; Hupp, J. T. *J. Phys. Chem.* **1995**, *99*, 2609.

(6) (a) Forlano, P.; Baraldo, L. M.; Olabe, J. A.; Della Vedova, C. O. *Inorg. Chim. Acta* **1994**, *223*, 37. (b) Forlano, P.; Cukiernik, F. D.; Poizat, O.; Olabe, J. A. *J. Chem. Soc., Dalton Trans.* **1997**, 1595. (c) Forlano, P.; Parise, A. R.; Videla, M.; Olabe, J. A. *Inorg. Chem.* **1997**, *36*, 5642. (d) Povse, V. G.; Olabe, J. A. *Transition Met. Chem.* **1998**, *23*, 657.

(7) (a) Endicott, J. F.; Song, X.; Watsky, M. A. *Chem. Phys.* **1993**, *176*, 427. (b) Watsky, M. A.; Macatangay, A. W.; Van Camp, R. A.; Mazzetto, S. E.; Song, X.; Endicott J. F.; Buranda, T. *J. Phys. Chem. A* **1997**, *101*, 8441.

(8) (a) Karki, L.; Lu, H. P.; Hupp, J. T. *J. Phys. Chem.* **1996**, *100*, 15637. (b) Karki, L.; Hupp, J. T. *J. Am. Chem. Soc.* **1997**, *119*, 4070. (c) Bublitz, G. U.; Laidlaw, W. M.; Denning, R. G.; Boxer, S. G. *J. Am. Chem. Soc.* **1998**, *120*, 6068.

(9) Vahrenkamph, H.; Geiss, A.; Richardson, G. N. *J. Chem. Soc., Dalton. Trans.* **1997**, 3643.

(10) (a) Rong, D.; Hong, H. G.; Kim, Y. I.; Krueger, J. S.; Mayer J. E.; Mallouk, T. E. *Coord. Chem. Rev.*, **1990**, *97*, 237. (b) Wu, Y.; Pfennig, B. W.; Bocarsly, A. B.; Vicenzi, E. P. *Inorg. Chem.*, **1995**, *34*, 4262.

(11) Laidlaw, W. M.; Denning, R. G.; Verbiest, T.; Chauchard, E.; Persoons, A. *Nature (London)*, **1993**, *363*, 58.

(12) (a) Comba, P. *Coord. Chem. Rev.* **1993**, *123*, 1. (b) Comba, P.; Sickmuller, A. F. *Inorg. Chem.* **1997**, *36*, 4500.

(13) (a) Lay, P. A. *J. Phys. Chem.* **1986**, *90*, 878. (b) Chang, J. P.; Fung, E. Y.; Curtis, J. C. *Inorg. Chem.* **1986**, *25*, 4233.

(14) (a) Drago, R. S. *Coord. Chem. Rev.* **1980**, *33*, 251. (b) Drago, R. S.; Richardson, D. E.; George, J. E. *Inorg. Chem.* **1997**, *36*, 25.

(15) Hupp, J. T.; Weaver, M. J. *Inorg. Chem.* **1984**, *23*, 256. Hupp, J. T.; Weaver, M. J. *Inorg. Chem.* **1984**, *23*, 3639.

(16) Sachinidis, J. I.; Shalders, R. D.; Tregloan, P. A. *Inorg. Chem.* **1994**, *33*, 6180. Sachinidis, J. I.; Shalders, R. D.; Tregloan, P. A. *Inorg. Chem.* **1996**, *35*, 2497.

(17) (a) Hush, N. S. *Prog. Inorg. Chem.* **1967**, *8*, 391. (b) Hush, N. S. *Electrochim. Acta* **1968**, ***13***, 1005. (c) Hush, N. S. *Chem. Phys.* **1975**, *10*, 361.

(18) (a) Curtis, J. C.; Meyer, T. J. *Inorg. Chem.* **1982**, *21*, 1562. (b) Brunschwig, B. S.; Ehrenson, S.; Sutin, N. *J. Phys. Chem.* **1986**, *90*, 3657.

(19) (a) Weaklein, H. A.; Hoard, J. L. *J. Am. Chem. Soc.* **1959**, *81*, 549. (b) Aochi, Y. O.; Sawyer, D. T. *Inorg. Chem.* **1966**, *5*, 2085.

(20) (a) Baisden, P. A.; Choppin, G. R.; Garrett, B. B. *Inorg. Chem.* **1977**, *16*, 1367. (b) Blixt, J.; Glaser, J.; Solomosi, P.; Tóth, I. *Inorg. Chem.* **1992**, *31*, 5288.

(21) (a) Agmon, N.; Hopfield, J. J. *J. Chem. Phys.* **1983**, *79*, 2042. (b) Agmon, N. *Biochemistry* **1988**, *27*, 3507. (c) Campbell, B. F.; Chance, M. R.; Friedman, J. M. *Science* **1987**, *238*, 373.

(22) Ormos, P.; Ansari, A.; Braunstein, D.; Cowen, B. R.; Frauenfelder, H.; Hong, M. K.; Iben, I. E.; Sauke, T. B.; Steinbach, P. J.; Young, R. D. *Biophys. J.* **1990**, *57*, 191.

(23) Khoshtariya, D. E.; Neubrand, A.; van Eldik, R. **1999**, manuscript in preparation.

(24) Furman, N. H.; Miller, C. O. *Inorg. Synth.* **1950**, *3*, 120.

(25) Spitzer, M.; Gartig, F.; van Eldik, R. *Rev. Sci. Instrument.* **1988**, *59*, 2092.

(26) (a) Billing, R.; Khoshtariya, D. E. *Inorg. Chem.* **1994**, *33*, 4038. (b) Khoshtariya, D. E.; Meusinger, R.; Billing, R. *J. Phys. Chem.* **1995**, *99*, 3592.

(27) (a) Marcus, R. A. *J. Chem. Phys.* **1957**, *26*, 867. (b) Marcus, R. A.; Sutin, N. *Biochim. Biophys. Acta* **1985**, *811*, 265. Marcus, R. A. *Comments Inorg. Chem.* **1986**, *5*, 119.

(28) (a) Khoshtariya, D. E.; Billing, R.; Ackermann, M.; van Eldik, R. *J. Chem. Soc., Faraday Trans.* **1995**, *91*, 1625. (b) Khoshtariya, D. E.; Neubrand, A.; van Eldik, R *Chem. Phys. Lett.* **1998**, *284*, 121.

(29) (a) Walrafen, G. E.; Fisher, M. R.; Hokmabadi, M. S.; Yang, W.-H. *J. Chem. Phys.* **1986**, *85*, 6970. (b) Walrafen, G. E.; Yang, W.-H.; Chu, Y. C.; Hokmabadi, M. S. *J. Phys. Chem.* **1996**, *100*, 1381.

(30) (a) Graener, H.; Seifert, G.; Lauberau, A. *Phys. Rev. Lett.* **1991**, *66*, 2092. (b) Graener, H.; Lauberau, A. *J. Phys. Chem.* **1991**, *95*, 3447. (c) Graener, H. *J. Phys. Chem.* **1991**, *95*, 3450.

(31) *The Chemical Physics of Ion Solvation*, Part A. Dogonadze, R. R., Kálmán, E., Kornyshev, A. A., Ulstrup, J., Eds.; Elsevier: Amsterdam, 1985.

(32) (a) Page, M. I.; Jencks, W. P. *Proc. Natl. Acad. Sci. U.S.A.* **1971**, *68*, 1678. (b) Page, M. I. *Chem. Soc. Rev.* **1973**, *2*, 295.

(33) The existence of direct hydrogen-bonding interactions in similar systems has been demonstrated by infrared spectroscopy in Casabo, J.; Ribas, J. *Inorg. Chim. Acta* **1977**, *21*, 5 (see also ref 18a).

(34) (a) Weakliem, H. A.; Hoard, J. L. *J. Am. Chem. Soc.* **1959**, *81*, 549. (b) Taqui Khan, M. M.; Bajaj, H. C.; Shirin, Z.; Venkatasubramanian, K. *Polyhedron* **1992**, *11*, 1059.

(35) (a) Matsubara, T.; Creutz, C. *Inorg. Chem.* **1979**, *18*, 1956. (b) Bajaj, H. C.; van Eldik, R. *Inorg. Chem.* **1989**, *28*, 1980. Bajaj, H. C.; van Eldik, R. *Inorg. Chem.* **1990**, *29*, 2855.